

Multispectral optoacoustic tomography of the human breast: characterisation of healthy tissue and malignant lesions using a hybrid ultrasound-optoacoustic approach

Anne Becker¹ · Max Masthoff¹ · Jing Claussen² · Steven James Ford² · Wolfgang Roll³ · Matthias Burg¹ · Peter J. Barth⁴ · Walter Heindel¹ · Michael Schäfers^{3,5} · Michel Eisenblätter^{1,6} · Moritz Wildgruber¹

Received: 16 February 2017 / Revised: 22 June 2017 / Accepted: 21 July 2017 / Published online: 7 August 2017
© European Society of Radiology 2017

Abstract

Background and aim Multispectral optoacoustic tomography (MSOT) represents a new in vivo imaging technique with high resolution (~250 µm) and tissue penetration (>1 cm) using the photoacoustic effect. While ultrasound contains anatomical information for lesion detection, MSOT provides functional information based on intrinsic tissue chromophores. We aimed to evaluate the feasibility of combined ultrasound/MSOT imaging of breast cancer in patients compared to healthy volunteers.

Methods Imaging was performed using a handheld MSOT system for clinical use in healthy volunteers (n = 6) and representative patients with histologically confirmed invasive breast carcinoma (n = 5) and ductal carcinoma in situ (DCIS, n = 2). MSOT values for haemoglobin and oxygen saturation

were assessed at 0.5, 1.0 and 1.5 cm depth and selected wavelengths between 700 and 850 nm.

Results Reproducible signals were obtained in all wavelengths with consistent MSOT signals in superficial tissue in breasts of healthy individuals. In contrast, we found increased signals for haemoglobin in invasive carcinoma, suggesting a higher perfusion of the tumour and tumour environment. For DCIS, MSOT values showed only little variation compared to healthy tissue.

Conclusions This preliminary MSOT breast imaging study provided stable, reproducible data on tissue composition and physiological properties, potentially enabling differentiation of solid malignant and healthy tissue.

Key Points

- A handheld MSOT probe enables real-time molecular imaging of the breast.
- MSOT of healthy controls provides a reproducible reference for pathology identification.
- MSOT parameters allows for differentiation of invasive carcinoma and healthy tissue.

Anne Becker and Max Masthoff contributed equally to this work.

Electronic supplementary material The online version of this article (doi:10.1007/s00330-017-5002-x) contains supplementary material, which is available to authorized users.

✉ Moritz Wildgruber
moritz.wildgruber@ukmuenster.de

¹ Department of Clinical Radiology, University Hospital Muenster, Albert-Schweitzer-Campus 1, A16, 49149 Muenster, Germany

² iThera Medical, Munich, Germany

³ Department of Nuclear Medicine, University Hospital Muenster, Muenster, Germany

⁴ Gerhard-Domagk-Institute of Pathology, University Hospital Muenster, Muenster, Germany

⁵ European Institute for Molecular Imaging – EIMI, University of Muenster, Muenster, Germany

⁶ Division of Imaging Sciences & Biomedical Engineering, King's College London, London, UK

Keywords Multispectral optoacoustic tomography · Optoacoustic imaging · Ultrasound · In vivo imaging · Breast cancer

Abbreviations

DCIS	Ductal carcinoma in situ
MRI	Magnetic resonance imaging
MSOT	Multispectral optoacoustic tomography
OA	Optoacoustic
PET	Positron emission tomography
ROI	Region of interest

RUCT Reflection ultrasound computed tomography
 US Ultrasound

Introduction

With a worldwide incidence of about 1.4 million per year, a lifetime risk of 7% and accounting for 14% of all cancer-related deaths, breast cancer is the most prevalent cancer in women and of major importance for both individual and national healthcare [1]. Various imaging modalities such as x-ray mammography, ultrasound (US), magnetic resonance imaging (MRI) or positron emission tomography (PET), also used as an indicator of therapeutic response [2], are commonly used in clinical diagnosis of breast cancer. Due to false-negative rates of up to 20%, especially with x-ray mammography, which remains the gold standard [3], further approaches have been introduced in recent studies to improve sensitivity and specificity of diagnosis. Using multimodal ultrasonic tomographic imaging, malignant breast lesions can be differentiated from healthy tissue and benign lesions by refractivity and frequency-dependent attenuation corresponding to compressibility and viscoelasticity of breast tissue [4]. However, specificity of diagnosis remains a main problem. To address this issue, shear-wave elastography was used as an adjunct to B-mode ultrasound to improve specificity of the assessment [5]. However, revealing tumour heterogeneity, tissue composition and vitality remains a challenge [6] as functional properties of breast tissue were not addressed by these approaches. Preliminary results of a two-dimensional (2D) diffuse optical imaging approach provided functional information reflected by greater light absorption due to higher total haemoglobin concentration in five breast cancer patients. However, the authors concluded that a second generation of the approach needs to overcome several limitations concerning limited tissue penetration, artefacts as well as detection of both oxygenated and deoxygenated Hb [3].

Multispectral optoacoustic tomography (MSOT) represents a promising new approach for non-invasive imaging as it enables depiction of tissue characteristics and biological parameters with high spatial resolution and without the need for extrinsic contrast agents [7, 8]. Compared to other optical imaging modalities, MSOT has good tissue penetration up to a few centimetres [7, 9, 10]. The MSOT principle is based on the photoacoustic effect, first described in 1881 [11]. Absorption of pulsed, high-energy light causes thermoelastic expansion of scanned tissue, inducing the transmission of US waves. Due to specific properties of intrinsic absorbers like haemoglobin, melanin or lipids, image reconstruction can reveal absorber distribution, which is expected to differ in physiological and pathological conditions [8, 12]. MSOT has been evaluated in several (pre-)clinical studies investigating vascular and cardiac [10, 13], oncological (especially malignant

melanoma) [14–16] and inflammatory diseases [17]. Regarding biological tissue properties of benign and malignant breast lesions, promising preclinical results have been reported using optical and photoacoustic imaging [18, 19].

Recently, a combined MSOT/US handheld approach for combined imaging of anatomical and functional properties has been developed and introduced [7, 9, 10]. Combining both imaging modalities overcomes previous limitations of MSOT concerning anatomical co-localisation, offering a higher potential for clinical translation.

We demonstrate the clinical applicability of a handheld optoacoustic/US scanner and provide the first evidence for an imaging signature associated with malignant versus healthy breast tissue.

Materials and methods

Technical description of MSOT imaging device

The clinical MSOT imaging system (MSOT Acuity Echo, iThera Medical, Munich) comprises a tunable optical parametric oscillator (OPO) that is pumped by an Nd:YAG laser to provide excitation pulses with a duration of 9 ns at wavelengths from 680 nm to 980 nm at a repetition rate 25 Hz and a peak pulse energy of 30 mJ at 730 nm. A handheld probe was used for MSOT imaging. This probe was connected to the OPO via a fibre bundle integrated into the probe with a diffuser providing an elliptical light spot of approximately 10 mm width and 15 mm length. The pulse energy was attenuated to ensure adherence with American National Standards Institute (ANSI) limits of maximum permissible exposure. The detector (256 transducer elements of centre frequency = 3 MHz; send/receive bandwidth = 56%; optoacoustic (OA) resolution ~250 μm) had a 125° angular coverage providing 2D cross-sectional images with a field of view (FOV) of 40 \times 40 mm² and 100 μm reconstructed pixel size. Multispectral images were acquired using one pulse per wavelength image. The MSOT penetration depth with the current setup was limited to 3 cm. The recorded images were reconstructed using a standard back-projection algorithm [20] after band-pass filtering and deconvolution with the electrical impulse response of the transducer. In order to partially compensate for light attenuation in tissue and to enhance the visualisation of deep structures, light fluence was modelled using exponential decay assuming $\mu_s = 15 \text{ cm}^{-1}$, $\mu_a = 0.022 \text{ cm}^{-1}$ at the isosbestic point (800 nm). To increase the signal-to-noise-ratio, a running average was applied over seven sequential frames if no detector movement was determined in the image sequence (Fig. 1A–C).

Reflection ultrasound computed tomography (RUCT)-mode US images were generated by the MSOT device using an US-imaging platform that consolidates transmit-receive boards and a function of triggered acquisition for

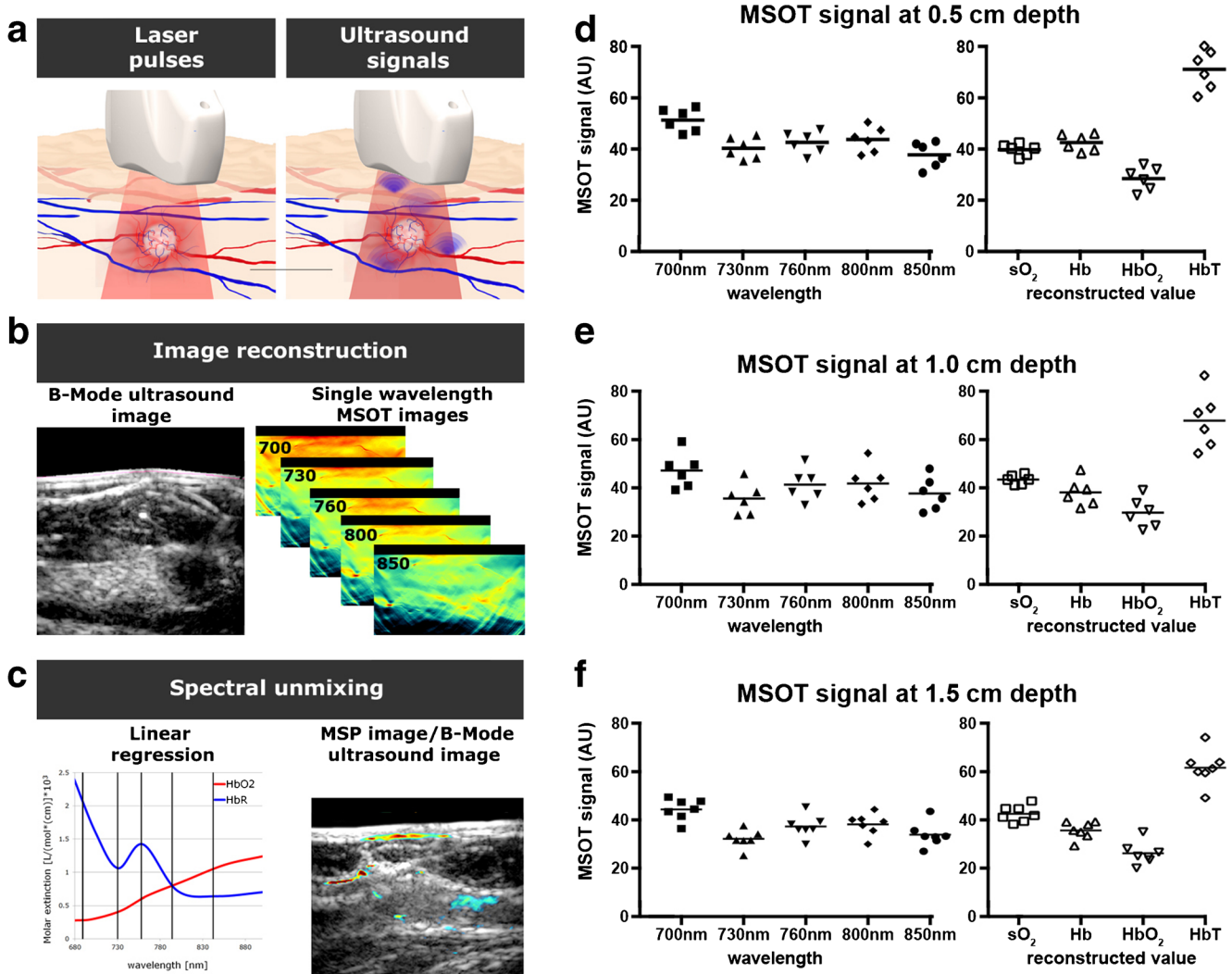


Fig. 1 The principle of multispectral optoacoustic tomography (MSOT) and imaging of healthy volunteers. Short pulses of light are absorbed by intrinsic tissue chromophores, inducing thermoelastic expansion and creating an ultrasound signal (A). Using multiple excitation wavelengths and tomographic signal detection, MSOT can spatially and

temporally resolve specific chromophores based on spectral unmixing methods (B, C). Comparison of MSOT signals (AU, 700–850 nm) from healthy individuals at different depths shows a trend in constant values with the most consistency at 0.5 cm depth, but more spread at 1.5 cm depth due to light scattering and absorption (D–F)

synchronising US and OA image streams, as previously described [21]. Generated transmit pulses had a peak-to-peak voltage of 20 V and a frequency of 5 MHz. Detected echo signals were reconstructed using transmit aperture technique at a FOV of $40 \times 40 \text{ mm}^2$ with a pixel size of $180 \mu\text{m}$ and a theoretical minimal US resolution of $345 \mu\text{m}$. US pulse-echo was applied in sub-apertures of one-quarter of the number detector elements (64 elements) with one single element continuously transmitting the pulse and all elements receiving the resulting echo signals. The single pulsing element swept across four sub-apertures and were combined to cover the entire angular coverage (256 elements) of the handheld array. The final image was generated by using spatial compounding of the sub-apertures.

MSOT image acquisition

MSOT images were acquired at five wavelengths: 700 nm, 730 nm, 760 nm, 800 nm and 850 nm. Individual contributions of oxygenated (HbO₂) and deoxygenated haemoglobin (HbR) were calculated from data acquired and based on their spectral absorption characteristics by spectral unmixing. Subsequently, total Hb (HbT = HbO₂ + HbR) and oxygen saturation ($s\text{O}_2 = \text{HbO}_2/\text{HbT}$) were calculated for regions of interest (ROIs) co-localised to structures identified on US images. MSOT values for each ROI represent the mean optoacoustic image value of all pixels. Subsequently, these MSOT parameters were pseudocolour-coded and visualised individually with the US image as background in composite images.

Measurements and patients

Initial examination with clinical MSOT was performed in healthy individuals ($n = 6$) using a handheld probe after obtaining written and informed consent of both healthy volunteers and breast cancer patients. Examinations were shorter than 15 min and eyes of examiners and patients were protected with laser safety goggles.

Measurements of both breasts were performed and ROIs (100 mm^2) were placed, based on the US images, at 0.5, 1.0 and 1.5 cm depth indicating results in arbitrary units (AU). Furthermore, breasts with histologically-confirmed malignant transformations were imaged on imaging data acquired in five patients with invasive breast cancer prior to surgical intervention. ROIs were placed in the tumour centre and tumour margin, depicted as hypoechogenic lesion in the corresponding US. Signals were compared with peritumoral tissue, co-localising with non-pathological findings in US, and unaffected breast tissue in the same patient at the same depth as the measured tumour lesions in intraindividual controls. As characteristically pathological US signals of ductal carcinoma in situ (DCIS, $n = 2$) do not exist, ROIs were defined in relation to ROIs of healthy controls. In both cases MRI revealed a diffuse infiltration of the entire breast by the DCIS, which was confirmed by histology upon complete mastectomy. Measurements of non-affected tissue served as intraindividual controls. For comparison, ratios (mean tumour/mean unaffected tissue) were calculated. ROIs covered 10 mm^2 (invasive carcinoma) and 100 mm^2 (DCIS).

Subsequently, results of MSOT imaging were compared to corresponding MRI and histological analyses (haematoxylin and eosin stain).

Statistical tests (unpaired t-test) and graphs were calculated using GraphPad Prism (version 7, GraphPad Software Inc.).

Results

The clinical MSOT imaging system enabled non-invasive real-time visualisation of the human breast. Parallel acquisition of RUCT-ultrasound and MSOT allowed for an exact anatomical co-localisation of physiological MSOT information enabling image fusion of pseudo colour-coded MSOT signals with US images. In the presented setup, individual images are reconstructed on the fly and refresh rate was possible at 25 Hz for single wavelength imaging. Multispectral imaging in this scenario is possible at up to 5 Hz (25 Hz * 5 WLs per multispectral image), and a 5Hz refresh rate per multispectral image.

Imaging of healthy controls

In healthy individuals, constant and reproducible MSOT signals with only little variation between single measurements

were detected at 0.5–1.5 cm depth. As expected, single-wavelength MSOT image intensities changed with wavelength (reflecting the absorbance profile of tissue chromophores), the variability in measurements was irrespective of imaging wavelength. Accordingly, the estimated values for Hb, HbO₂, HbT and sO₂ were reproducibly stable in the healthy tissue. With increasing tissue depth, MSOT signals showed an overall reduction of mean values and greater spread due to light scattering and absorption (Fig. 1D-F).

Imaging of malignancies

In comparison to unaffected breast tissue and peritumoral tissue, MSOT of invasive carcinoma showed increased signals for Hb, HbO₂ and HbT. Calculated tumour-control ratios for deoxygenated Hb showed a significant increase in tumour centre (1.13, SD = 0.03, $p = 0,019$) and tumour margin (1.07, SD = 0.06, $p = 0,031$), each compared with peritumoral tissue (Fig. 2A). Accordingly, ratios for HbT were significantly increased in both the tumour centre (1.18, SD = 0,04, $p = 0,002$) and the tumour margin (1.13, SD = 0.04, $p = 0,007$) compared with peritumoral tissue (Fig. 2C). Calculated sO₂ ratios revealed no significant differences (calculated ratios: 1.03 for tumour centre, 1.03 for peritumoral tissue, Fig. 2D).

Thus, similar sO₂ but increased Hb signals in the tumour centre suggest higher tumour perfusion compared with healthy tissue due to tumour neovascularisation and tumour-associated inflammation in the surrounding tissue. Accordingly, the MSOT signal was most elevated in the centre and margin of the tumour lesion (Fig. 2E). MSOT results were supplemented with MRI images, which showed gadolinium enhancement exemplarily in a lesion of the right breast with irregular margins (Fig. 2F). Diagnosis was corroborated by postoperative histology confirming invasive breast carcinoma (Fig. 2G).

MSOT ratios for all parameters showed no obvious increase in the two DCIS cases when compared to healthy breast tissue (mean Hb: 1.02, mean HbO₂: 1.07 and mean HbT: 1.038, Fig. 3A,B). However, a non-mass, diffuse gadolinium enhancement was detected in all quadrants of the left breast by MRI (Fig. 3C) and cancerous infiltration of the entire breast by the DCIS was confirmed by histology after mastectomy (Fig. 3D).

There was no relevant operator dependency noted for handheld MSOT of breast carcinoma (Supplementary Fig. 1).

Discussion

The possibility of assessing physiological and molecular properties of a tumour non-invasively during regular screening and staging examinations would facilitate current cancer care. The impact of tumour hypoxia, neovascularisation and the tumour environment on tumour growth and metastasis has

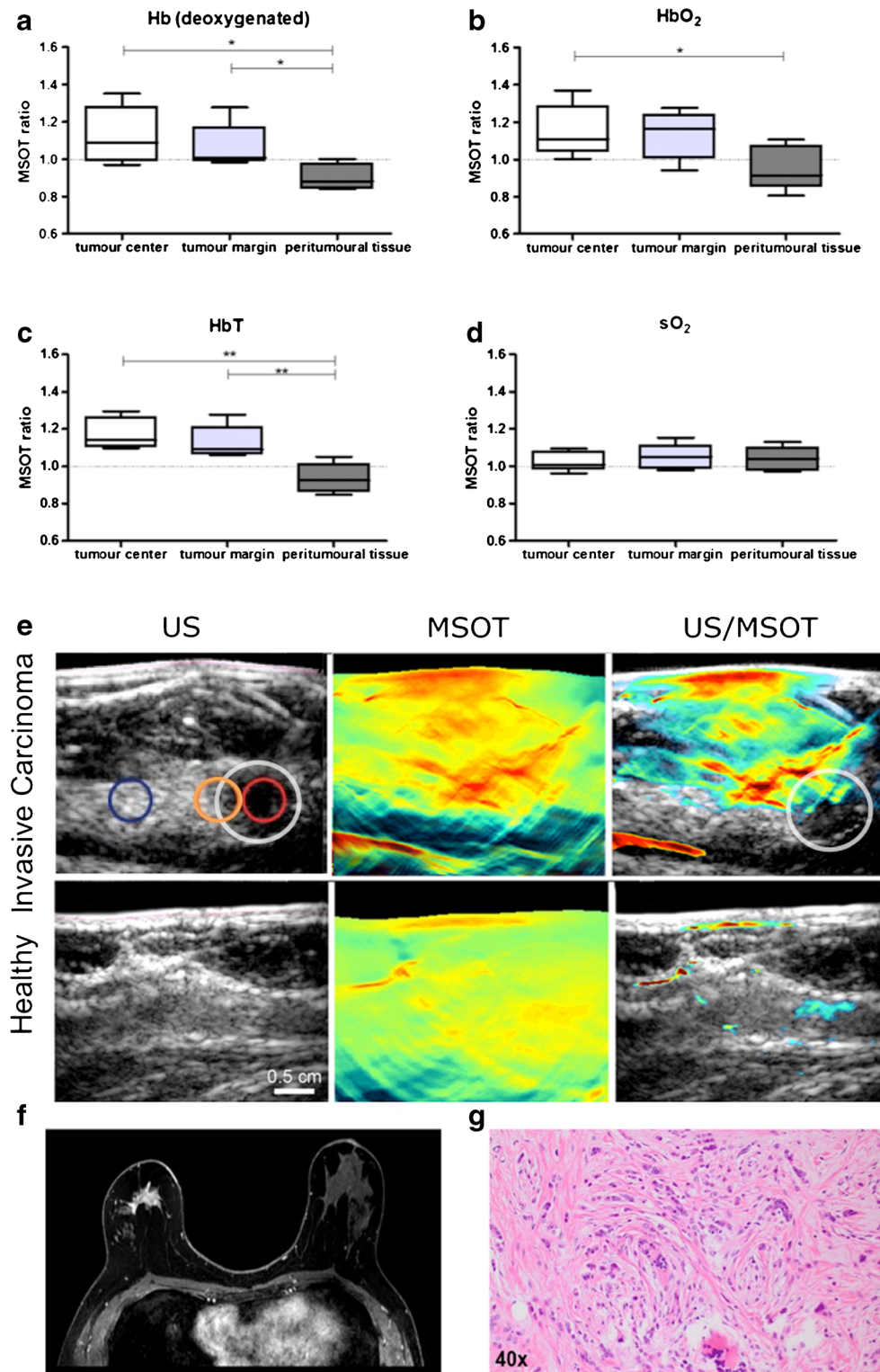


Fig. 2 Clinical multispectral optoacoustic tomography (MSOT) of invasive carcinoma. In invasive carcinoma ($n = 5$) significantly increased tumour-control ratios for Hb ($p = 0,019$), HbO₂ ($p = 0,043$) and HbT ($p = 0,002$) were approximated in the tumour centre (red) compared with peritumoural tissue (blue, A–C). Comparison of calculated ratios in the tumour margin (orange) and peritumoural tissue showed significantly higher ratios for Hb ($p = 0.031$) and HbT ($p =$

0.007 , A,C) No significant differences could be detected for oxygen saturation (D). Elevated MSOT signals could be detected in an exemplary MSOT-ultrasound image overlay with highlighted tumour lesion (white circle, E). Gadolinium enhancement was found in co-localisation in a corresponding MRI (T1 post gadolinium, D), diagnosis of invasive carcinoma was confirmed by histological analysis (haematoxylin and eosin stain, E)

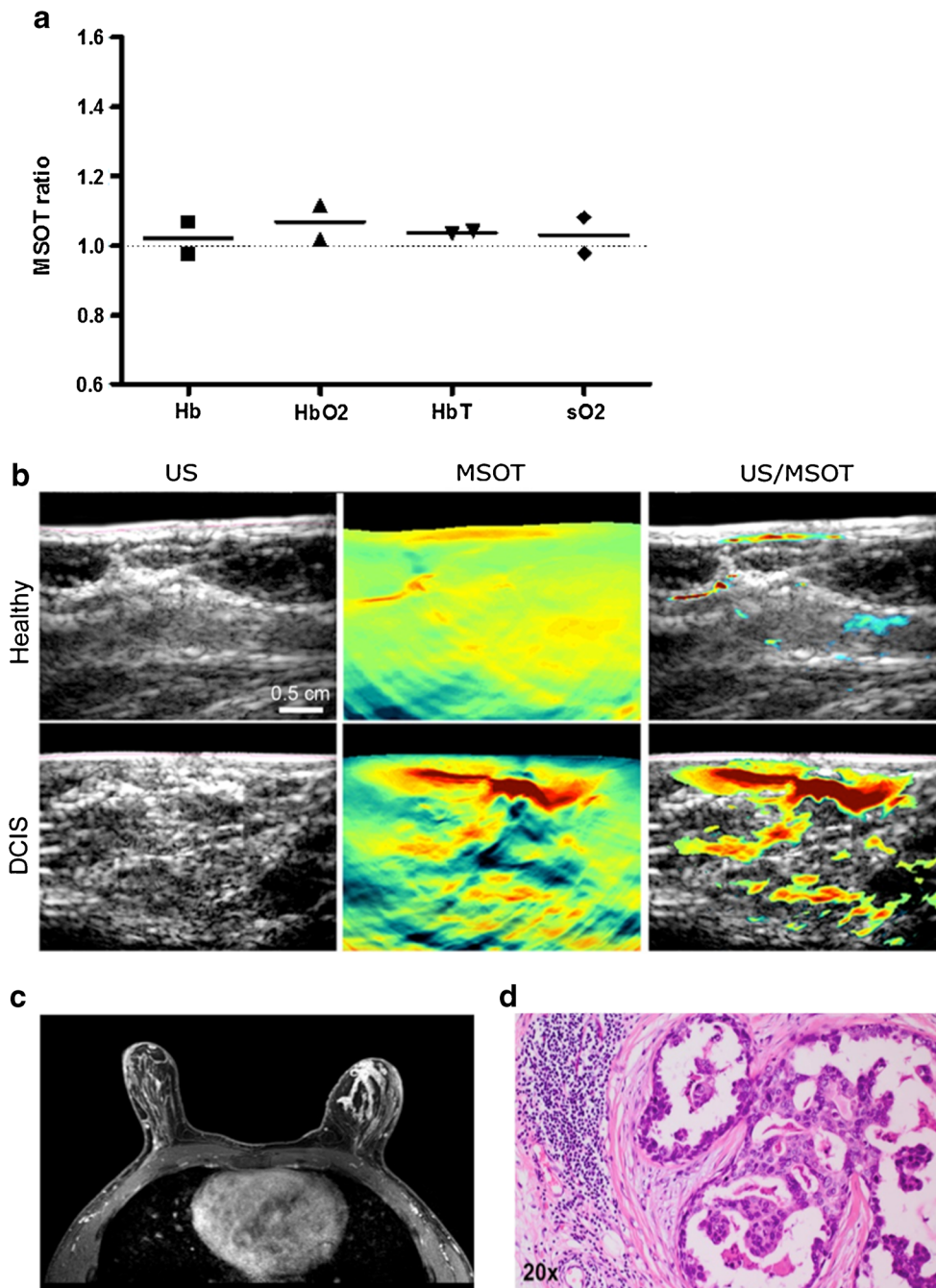


Fig. 3 Clinical multispectral optoacoustic tomography (MSOT) of ductal carcinoma in situ (DCIS). For MSOT measurements of DCIS patients (n = 2) tumour-control ratios for Hb, HbO₂, HbT and sO₂ were calculated. Ratios were similar between healthy tissue and DCIS. Furthermore no significant differences could be detected between

tumour and peritumoral tissue (A). Exemplary MSOT signals were relatively diffuse distributed in correlating areas (B). Non-mass gadolinium enhancement was, however, detected in all quadrants of the left breast via MRI (T1 post gadolinium, C) and was confirmed by histology after mastectomy (haematoxylin and eosin stain, D)

been previously described for breast cancer [22–26]. MSOT offers semi-quantitative assessment of such functional parameters via distinction between different intrinsic absorbers (haemoglobin, melanin, lipids etc.) and has proven to be a promising approach in various applications, with only a recent emergence of clinical studies [9, 10, 13, 16, 17]. In preliminary

experimental studies first photoacoustic image patterns of breast cancer have been described using the Twente Mammoscope [27]. Here we evaluated in a feasibility study for human breast whether clinical MSOT is (1) applicable, (2) reproducible and comparable within individuals scanned, and (3) allows distinction between healthy and malignant tissue in vivo.

As US is an established imaging procedure, the hybrid US/MSOT handheld probe is simple to use in the clinical setting and examinations proved to be quick, performed within the same timeframe as US imaging. MSOT measurements of healthy tissue were reproducible and interindividually comparable with low variance within our study group (Fig. 1). Thus, our results show first evidence for an imaging signature that may be representative of healthy breast tissue. Values obtained from healthy individuals may serve as a baseline for assessment of disease as well as monitoring of therapeutic approaches.

Clinical MSOT characterised tissue properties within invasive carcinoma formation: deoxygenated and oxygenated and especially total haemoglobin were increased in the tumour centre and margin when compared to healthy tissue, suggesting high perfusion and neovascularisation. However, the oxygen saturation was not significantly increased. Similar findings of elevated perfusion but low oxygen saturation in invasive carcinoma have been described previously [18, 19, 26, 28, 29]. The results can be interpreted as an indicator of intratumoral heterogeneity and potentially aid the characterisation of tumour composition.

Only a small increase in MSOT signals in DCIS could be a correlate of inhomogeneous tissue composition with both oxygenated and deoxygenated areas/increased and decreased perfusion within the same intratumoral ROI. Analysis of additional (intrinsic) parameters like lipids might help to further understand tissue characterisation and differentiation.

Our initial study comprises only a limited, exemplary number of samples but is thought to serve as a paradigm and inspiration for future study cohorts of relevant size. In addition, we acknowledge the use of a simple fluence correction method to correct for the attenuation of light with imaging depth. Despite this assumption, ROI analysis showed consistent results at multiple imaging depths in healthy tissue. Furthermore, ROI analysis was performed at similar depths in the breast carcinoma cases to minimise the effects introduced by shortcomings of fluence assumptions on the measured MSOT values. Furthermore, advances in system technology, image reconstruction and unmixing algorithms are expected to improve device performance by increasing tissue penetration for detecting deep lesions and specificity of absorber detection [8, 12]. Operator dependency of combined US/optoacoustic imaging may also have a potential impact for the MSOT results, and this needs to be further investigated in larger patient cohorts.

In summary, we demonstrate the feasibility of hybrid acquisition of US and MSOT signal with a handheld probe, enabling non-invasive clinical breast imaging with consistent, reproducible acquisition of anatomical and functional information. We anticipate that these findings will contribute to continuously translating MSOT imaging into the clinics. We believe that

non-invasive tissue characterisation in breast cancer is of great benefit for development of personalized breast cancer care.

Compliance with ethical standards

Guarantor The scientific guarantor of this publication is Moritz Wildgruber.

Conflict of interest The authors of this manuscript declare relationships with the following companies:

Jing Claussen and Steven J. Ford are employees of iThera Medical, a manufacturer of commercial optoacoustic scanners.

Funding The authors state that this work has not received any funding.

Statistics and biometry One of the authors has significant statistical expertise.

No complex statistical methods were necessary for this paper.

Informed consent Written informed consent was obtained from all subjects (patients) in this study.

Ethical approval Institutional Review Board approval was waived because scans were obtained during a pilot test series, which was covered under the Declaration of Helsinki §37 ('individual healing research')

Methodology

- prospective
- experimental
- performed at one institution

References

1. Jemal A, Bray F, Center MM, Ferlay J, Ward E, Forman D (2011) Global cancer statistics. *CA Cancer J Clin* 61:69–90
2. Shankar LK, Hoffman JM, Bacharach S et al (2006) Consensus recommendations for the use of 18F-FDG PET as an indicator of therapeutic response in patients in National Cancer Institute Trials. *J Nucl Med* 47:1059–1066
3. Erickson-Bhatt SJ, Roman M, Gonzalez J, et al (2015) Noninvasive surface imaging of breast cancer in humans using a hand-held optical imager. *Biomed Phys Eng Express* 1(4). doi:10.1088/2057-1976/1/4/045001
4. Zografos G, Liakou P, Koulocheri D et al (2015) Differentiation of BIRADS-4 small breast lesions via Multimodal Ultrasound Tomography. *Eur Radiol* 25:410–418
5. Berg WA, Cosgrove DO, Dore CJ et al (2012) Shear-wave elastography improves the specificity of breast US: the BE1 multinational study of 939 masses. *Radiology* 262:435–449
6. Song JL, Chen C, Yuan JP, Sun SR (2016) Progress in the clinical detection of heterogeneity in breast cancer. *Cancer Med* 5:3475–3488
7. Buehler A, Kacprowicz M, Taruttis A, Ntziachristos V (2013) Real-time handheld multispectral optoacoustic imaging. *Opt Lett* 38: 1404–1406
8. Valluru KS, Willmann JK (2016) Clinical photoacoustic imaging of cancer. *Ultrasonography* 35:267–280
9. Dima A, Ntziachristos V (2016) In-vivo handheld optoacoustic tomography of the human thyroid. *Photoacoustics* 4:65–69
10. Taruttis A, Timmermans AC, Wouters PC, Kacprowicz M, van Dam GM, Ntziachristos V (2016) Optoacoustic imaging of human

- vasculature: feasibility by using a handheld probe. *Radiology* 281: 256–263
11. Bell AG (1881) The production of sound by radiant energy. *Science* 2:242–253
 12. Taruttis A, Ntziachristos V (2015) Advances in real-time multispectral optoacoustic imaging and its applications. *Nat Photonics* 9: 219–227
 13. Taruttis A, Wildgruber M, Kosanke K et al (2013) Multispectral optoacoustic tomography of myocardial infarction. *Photoacoustics* 1:3–8
 14. McCormack D, Al-Shaer M, Goldschmidt BS et al (2009) Photoacoustic detection of melanoma micrometastasis in sentinel lymph nodes. *J Biomech Eng* 131, 074519
 15. McNally LR, Mezera M, Morgan DE et al (2016) Current and emerging clinical applications of Multispectral Optoacoustic Tomography (MSOT) in Oncology. *Clin Cancer Res* 22:3432–3439
 16. Neuschmelting V, Lockau H, Ntziachristos V, Grimm J, Kircher MF (2016) Lymph node micrometastases and in-transit metastases from melanoma: in vivo detection with multispectral optoacoustic imaging in a mouse model. *Radiology* 280:137–150
 17. Bhutiani N, Grizzle WE, Galandiuk S et al (2016) Non-invasive imaging of colitis using multispectral optoacoustic tomography. *J Nucl Med* 58:1009–1012
 18. Grosenick D, Rinneberg H, Cubeddu R, Taroni P (2016) Review of optical breast imaging and spectroscopy. *J Biomed Opt* 21, 091311
 19. Tromberg BJ, Shah N, Lanning R et al (2000) Non-invasive in vivo characterisation of breast tumors using photon migration spectroscopy. *Neoplasia* 2:26–40
 20. Xu M, Wang LV (2005) Universal back-projection algorithm for photoacoustic computed tomography. *Phys Rev E Stat Nonlin Soft Matter Phys* 71, 016706
 21. Mercep E, Burton NC, Claussen J, Razansky D (2015) Whole-body live mouse imaging by hybrid reflection-mode ultrasound and optoacoustic tomography. *Opt Lett* 40:4643–4646
 22. Folkman J (1994) Angiogenesis and breast cancer. *J Clin Oncol* 12: 441–443
 23. Vaupel P, Hockel M (2000) Blood supply, oxygenation status and metabolic microenvironment of breast cancers: characterisation and therapeutic relevance. *Int J Oncol* 17:869–879
 24. Becker A, Grosse-Hokamp N, Zenker S et al (2015) Optical in vivo imaging of the alarmin S100A9 in tumor lesions allows for estimation of the individual malignant potential by evaluation of tumor-host cell interaction. *J Nucl Med* 56:450–456
 25. Gilkes DM, Semenza GL (2013) Role of hypoxia-inducible factors in breast cancer metastasis. *Future Oncol* 9:1623–1636
 26. Ham M, Moon A (2013) Inflammatory and microenvironmental factors involved in breast cancer progression. *Arch Pharm Res* 36: 1419–1431
 27. Heijblom M, Piras D, Brinkhuis M et al (2015) Photoacoustic image patterns of breast carcinoma and comparisons with Magnetic Resonance Imaging and vascular stained histopathology. *Sci Rep* 5: 11778
 28. Ntziachristos V, Yodh AG, Schnall MD, Chance B (2002) MRI-guided diffuse optical spectroscopy of malignant and benign breast lesions. *Neoplasia* 4:347–354
 29. Enfield LC, Gibson AP, Hebden JC, Douek M (2009) Optical tomography of breast cancer-monitoring response to primary medical therapy. *Target Oncol* 4:219–233